Electronic Supplementary Material (ESI) for Journal of Materials Chemistry B.

Supplementary Information

Osteogenesis regulation of mesenchymal stem cells *via* autophagy induced by Silica-Titanium composite surfaces with different mechanical modulus

Maowen Chen[a], Yan Hu[a],*, Yanhua Hou[b], Menghua Li[c], Maohua Chen[a], Lu Tan[a], Caiyun Mu[a], Bailong Tao[a], Zhong Luo[c],*, Kaiyong Cai[a],*

[a]Key Laboratory of Biorheological Science and Technology, Ministry of Education, College of Bioengineering, Chongqing University, Chongqing 400044, China.

[b]Engineering Research Centre of Pharmaceutical Sciences, Chongqing Medical and Pharmaceutical College, Chongqing 401331, P. R. China.

[c]School of Life Science, Chongqing University, Chongqing 400044, China

*Corresponding author: professor Yan Hu, Zhong Luo & Kaiyong Cai

E-mail: huyan303@cqu.edu.cn; luozhong918@cqu.edu.cn; kaiyong_cai@cqu.edu.cn.

Additional data:

Synthesis of nanoparticles (SSN4, SSN5 and SSN10): The silica nanoparticles were synthesized *via* a Stober method. Briefly, silica nanoparticles of 400 nm, 500 nm and 1000 nm were synthesized by adjusting concentrations of water and ammonia in ethanol with the 0.28 M of tetraethyl silicate as the follows: [H2O] / [NH_3] = 15:7, [H2O] / [NH_3] = 12.5:7, [H2O] / [NH_3] = 1. Finally, the ultimate products were dried at 60 °C for further use.

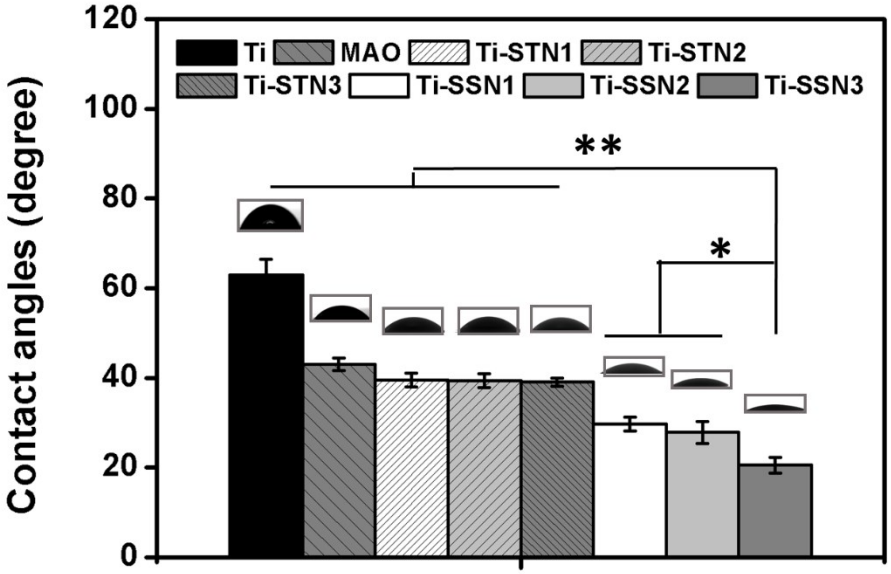

Figure S1. Wetting angle of different samples. Error bars represent means ± SD, n=3, *$^{**}p < 0.01$, $^{*}p < 0.05$.

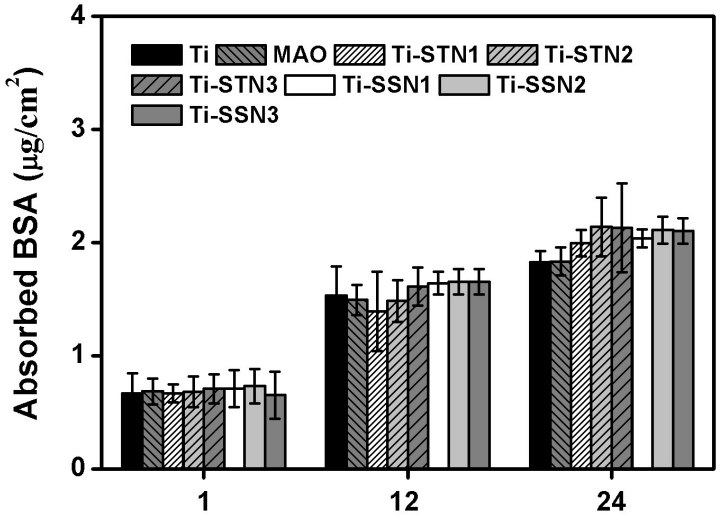

Figure S2. The adsorption behaviors (FBS) on the surfaces of Ti, MAO, Ti-SSN and Ti-STN respectively. Error bars represent means SD, n = 3.

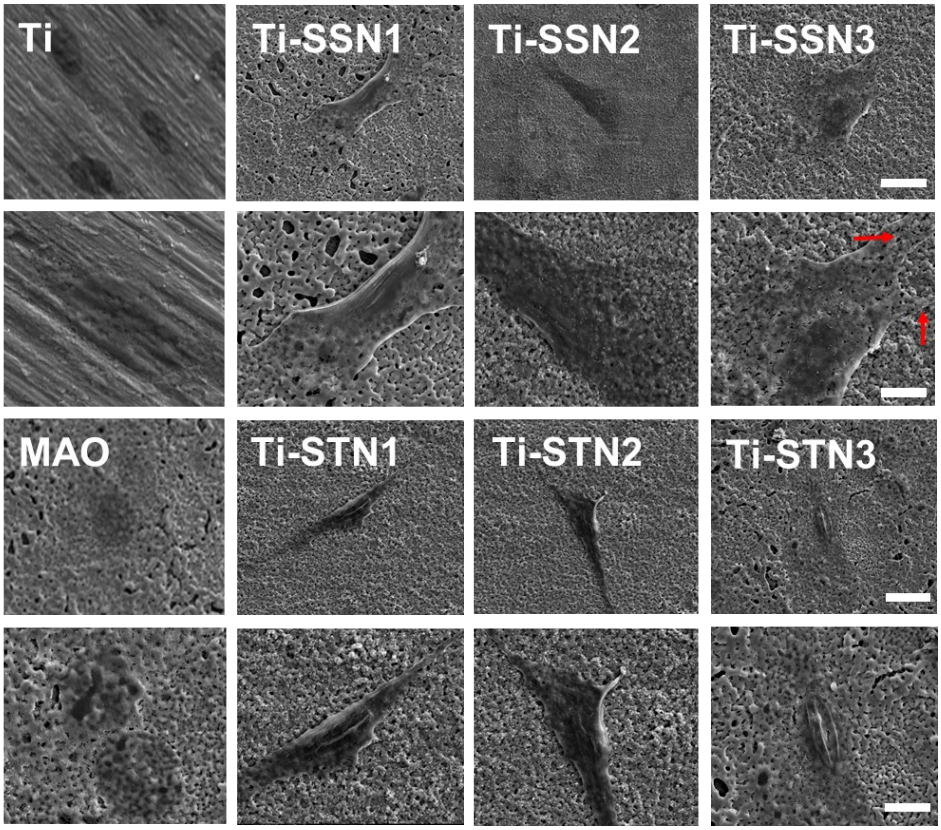

Figure S3. (A) SEM images of MSCs cultured on different substrates: Pseudopodia of MSCs were marked with red arrows. Scale bar: 10 μm.

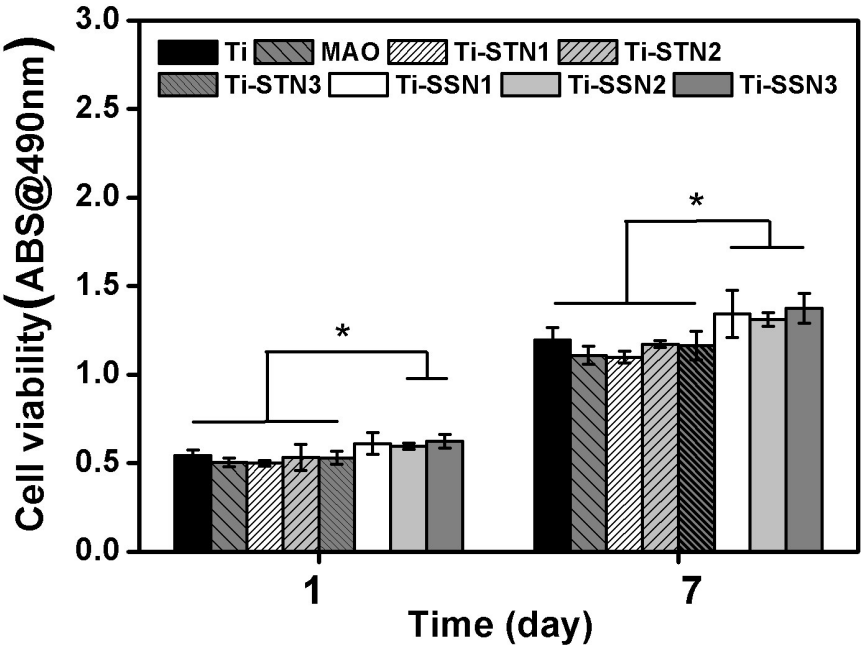

Figure S4. Cell viability of MSCs treated with various substrates and normal DMEM medium for 1 and 7 d, respectively. Error bars represent means ± SD, n=3, *$p < 0.05$.

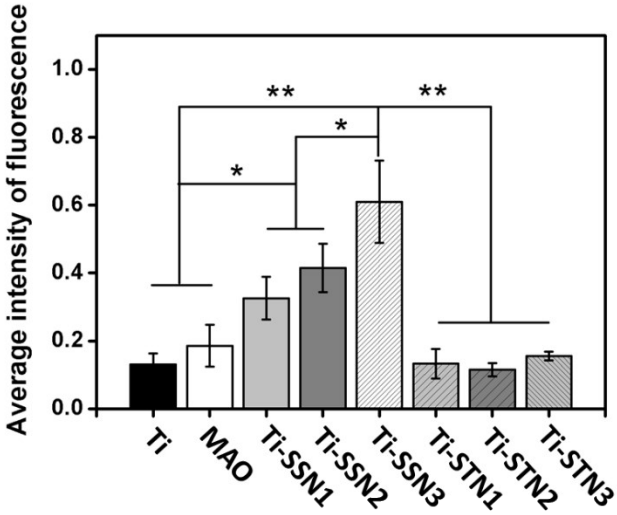

Figure S5. Average intensity of fluorescence statistics. Error bars represent means ± SD, n=3, *$p < 0.05$.

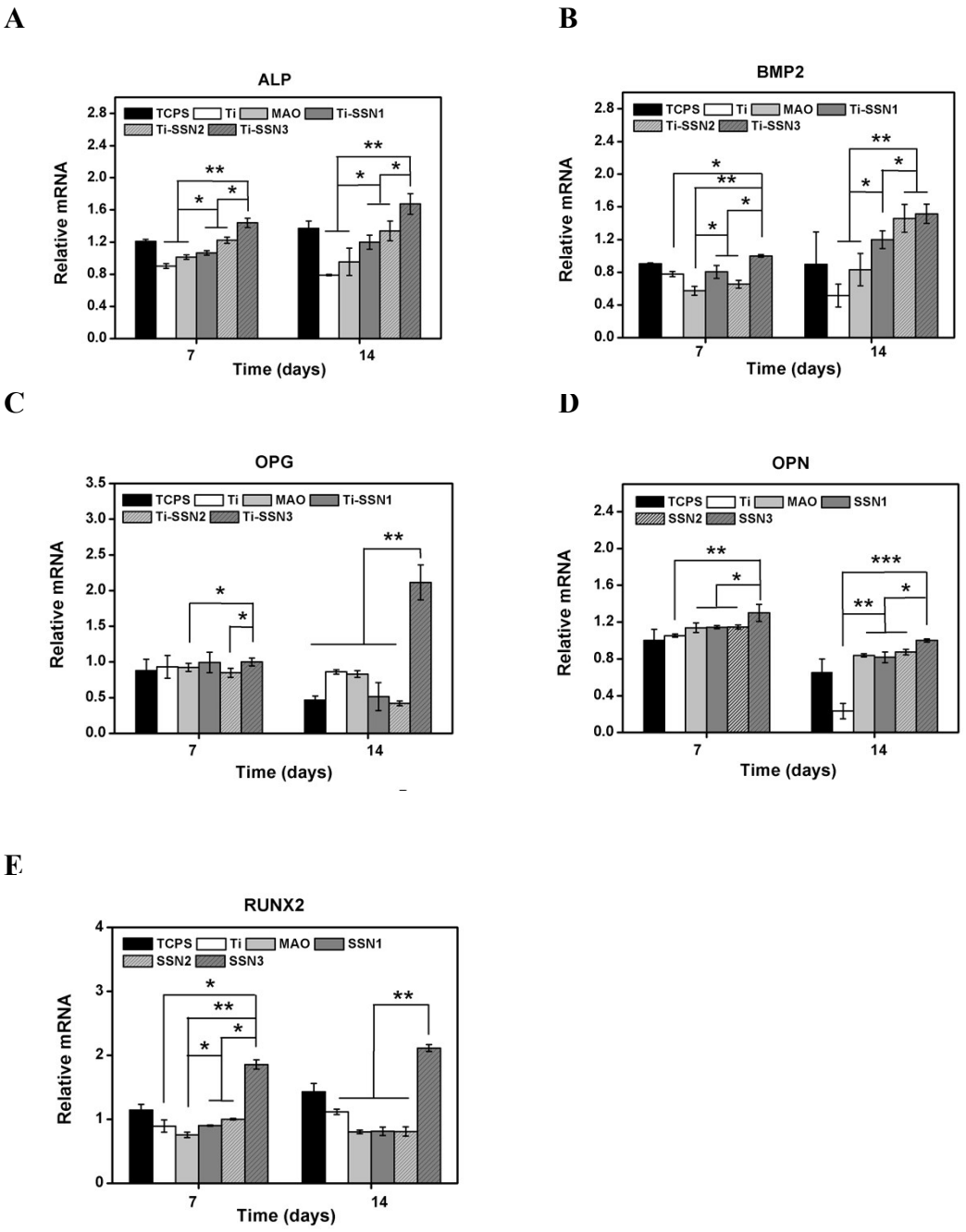

Figure S6. Relative mRNA expression of osteogenesis- related genes (ALP, OPG, BMP2, RUNX2 and OPN) in MSCs treated with various samples for 7 and 14 d, respectively. Error bars represent means ± SD, n=3, $^{**}p < 0.01, ^{*}p < 0.05$.

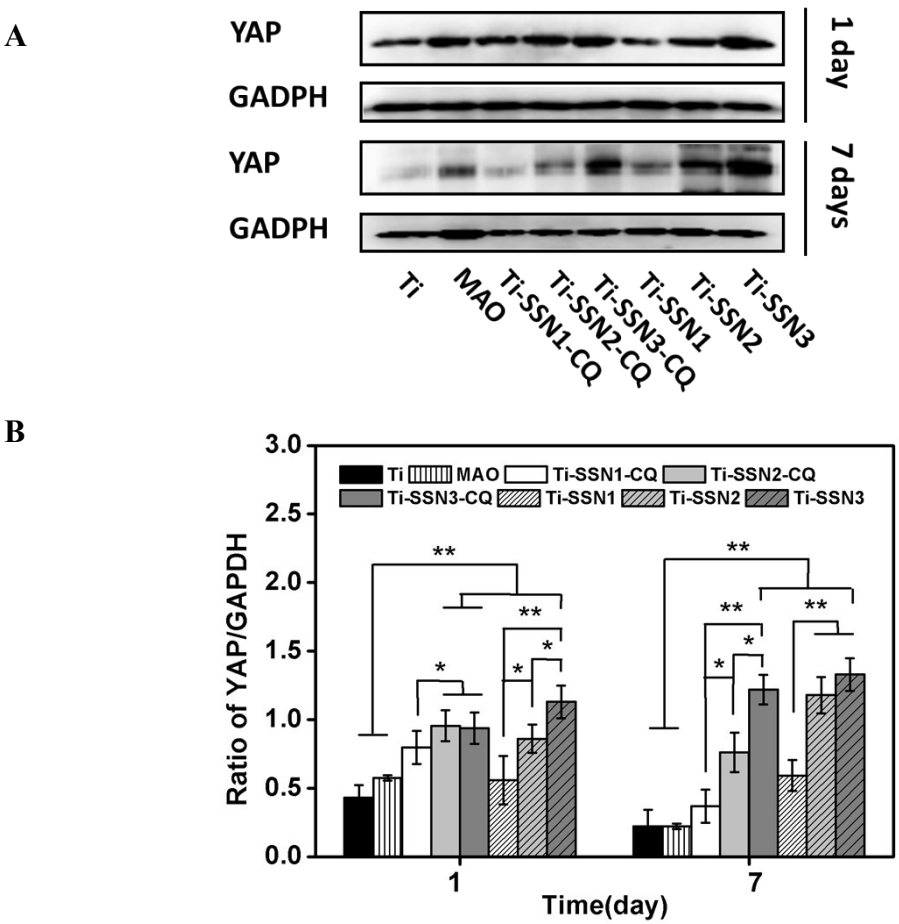

Figure S7. Representative Western blotting of YAP in MSCs treated with all samples with or without autophagy inhibitor (CQ) for 1 and 7 d.

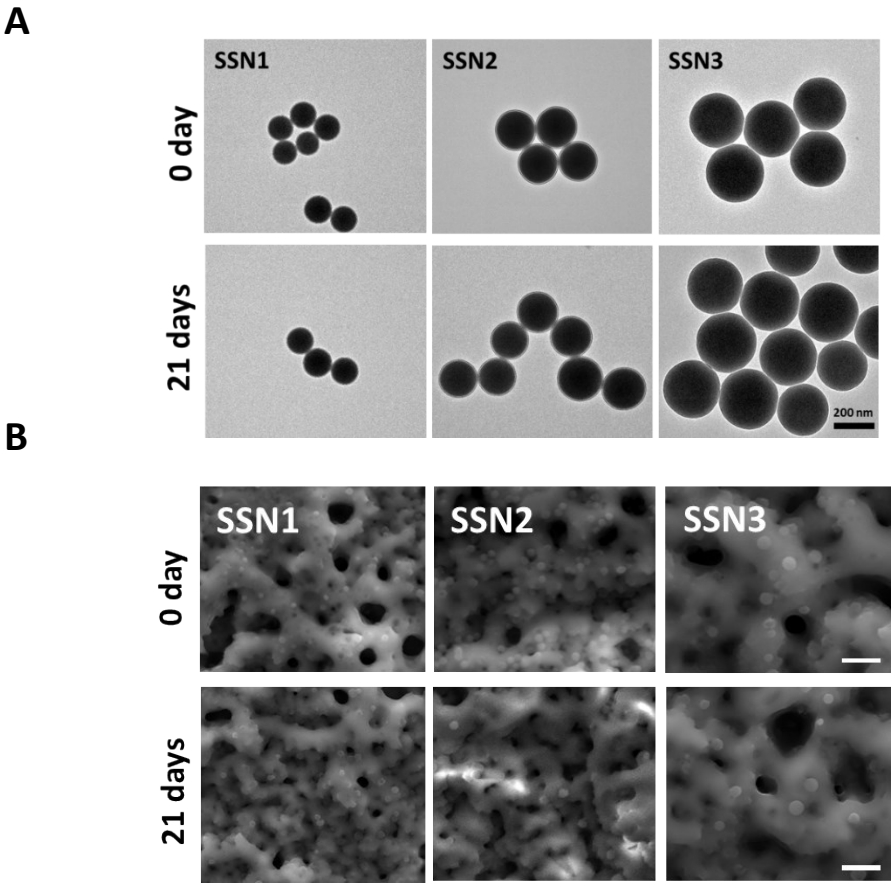

Figure S8. Long-term stability of these nanoparticles in culture medium. (A) These nanoparticles were incubated in normal culture medium for 21 days and then observed with TEM (Scale bar: 200 nm); (B) Different Ti substrates were incubated in normal culture medium for 21 days and then observed with SEM (Scale bar: 2 μm).

We synthesized spherical silica nanoparticles with different sizes to investigate their biodegradation capability using TEM. As shown in Fig. S8A, after incubated into normal culture medium (DMEM with low glucose supplemented with 10% FBS (fetal bovine serum) for 21 days, the structures of the three types of silica nanoparticles remained intact and the boundaries of the nanoparticles were relatively clear. This result showed that the silica nanoparticles were stable in biologically relevant conditions. Similarly, when the silica nanoparticles were embedded into titanium (Ti-SSNs) by MAO technique, the structures of three types of different Ti-SSN substrates have also

been well maintained after incubating in normal culture medium for 21 days (shown in Fig. S8B). These results demonstrated that the amount of silicon ion/silicate leakage was negligible in biological fluids, thus leading to minimal impacts on cell behaviors.

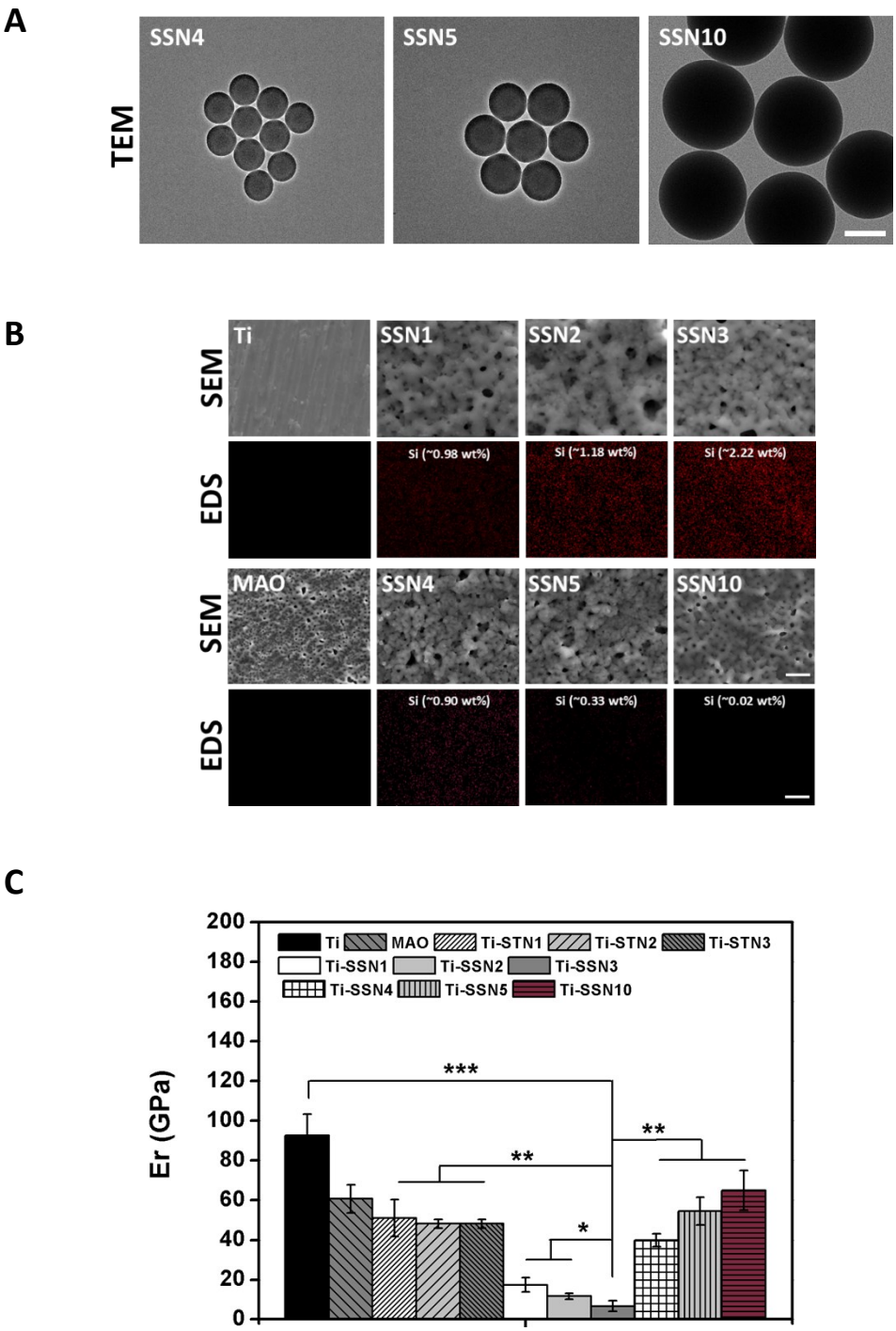

Figure S9. (A) Morphological characterizations of the TEM images of SSN4, SSN5 and SSN10 (scale bar: 500 nm); (B) SEM and EDS images of different Ti substrates (scale bar: 2 μm); (C) Elastic modulus statistics of SSN and STN groups.

We have synthesized SSN4, SSN5 and SSN10 corresponding to the diameter of 400 nm, 500 nm and 1 μm (Fig. S9A and also loaded onto Ti surfaces via micro-arc oxidation (MAO) technique. Considering the mechanistic properties of the MAO process, large-size particles were more difficult to be integrated into the oxidative coating due to the higher resistance in the electrolyte. Therefore, it's anticipated that the amount of silica introduced on to the titanium surface may decrease when the nanoparticle size increased above a certain threshold. As shown in the Fig. S9B, when the particle size was greater than 300 nm, the silica content on the surface of titanium decreased sharply. Particularly, for nanoparticles with the size of 1 μm there was almost no silica on the Ti surface. As shown in the Fig. S9C, it was noted that the surface modulus of Ti-SSN4, Ti-SSN5 and Ti-SSN10 were 39.8±3.3 GPa, 54.54±7.1 GPa and 65.0±10 GPa, respectively, which showed no apparent reduction in surface elasticity.

Table S1. Real-time polymerase chain reaction primers used in this study.

Samples	*Elemental content (wt %)*				
	Ti	O	P	C	Si
Ti	96.1 ± 1.1	—	—	5.05± 0.2	—
MAO	43.8 ± 0.9	43.6 ± 1.8	7.1 ± 0.5	2.36 ± 0.3	—
Ti-SSN1	49.8 ± 1.4	45.8 ± 0.9	6.3 ± 0.7	2.07 ± 0.1	1.22 ± 0.1
Ti-SSN2	44.8 ± 0.8	43.45 ± 1.0	6.49 ± 0.5	2.91 ± 0.2	1.96 ± 0.1
Ti-SSN3	43.1 ± 0.2	43.3 ± 1.1	7.43 ± 0.5	3.02 ± 0.2	2.34 ± 0.2
Ti-STN1	49.8 ± 3.4	39.16 ± 0.9	8.37 ± 1.9	2.42 ± 0.2	—
Ti-STN2	48.7 ± 0.4	40.9 ± 0.6	7.87 ± 0.5	2.55 ± 0.2	—
Ti-STN3	50.0 ± 0.7	39.5 ± 1.3	8.13 ± 0.6	2.30 ± 0.1	—

Table S2. Real-time polymerase chain reaction primers used in this study.

Target gene	*Primers*	*Product size (bp)*
ALP	AGCGACACGGACAAGAAGC	183
	GGCAAAGACCGCCACATC	
OPG	GCCCAGACGAGATTGAGAG	173
	CAGACTGTGGGTGACGGTT	
OPN	GACAGCAACGGGAAGACC	216
	CAGGCTGGCTTTGGAACT	
OCN	AGATTGTTGGGGCACAAGGT	191
	CCTTCAGCAGGGAAACCGAT	
Runx2	GCCGTAGAGAGCAGGGAAGAC	150
	CTGGCTTGGATTAGGGAGTCAC	
GAPDH	GGCATTGCTCTCAATGACAA	223
	TGTGAGGGAGATGCTCAGTG	